

# Validation of a quasilinear turbulent transport model in ASDEX Upgrade sawtoothing plasmas

F. Stefanelli<sup>1\*</sup>, G. Lo-Cascio<sup>1</sup>, E. Fable<sup>1</sup>, C. Angioni<sup>1</sup>, H. Zohm<sup>1</sup> and the ASDEX Upgrade team<sup>2</sup>

<sup>1</sup>Max Planck Institute for Plasma Physics, 85748 Garching, Germany

<sup>2</sup>See author list of T. Pütterich *et al* 2026 *Nucl. Fusion*, **66**, 116002 <https://doi.org/10.1088/1741-4326/ae61c8>

## Abstract

The predictions of TGLF-SAT2 at the  $q = 1$  surface of an ASDEX Upgrade discharge are compared to linear GENE calculations. Both TGLF default settings and settings aiming at better capturing Kinetic Ballooning modes (KBMs) are tested. It is found that TGLF with KBM settings agrees with GENE better than with the default settings for  $k_y \rho_s > 0.1$ , as TGLF with default settings calculates growth rates up to one order of magnitude smaller than those of GENE. However, TGLF with KBM settings predicts modes with large growth rates and frequencies at  $k_y \rho_s < 0.1$ , which are not found by GENE. Even by excluding modes at  $k_y \rho_s < 0.15$ , TGLF with KBM settings predicts turbulent fluxes one order of magnitude larger than those of TGLF with default settings, due to the small growth rates found in the latter case. Both versions of TGLF are then tested within a recently developed integrated model of sawtooth cycles and validated on an ASDEX Upgrade discharge, with  $k_y \rho_s \geq 0.15$  for the case with KBM settings. While the simulations with the default settings of TGLF yield an excellent agreement with the experimental results, the good agreement between TGLF with KBM settings and GENE for  $k_y \rho_s \geq 0.15$  hints at turbulent stabilisation mechanisms missing in the models, which are only compensated by the low growth rates obtained by TGLF with default settings.

## 1. Introduction

Sawtooth cycles are periodic relaxations of the core plasma kinetic and current profiles commonly observed in tokamak discharges [1]. These oscillations are characterised by a rapid crash of the core density, temperature and current profiles. The underlying mechanism of sawtooth dynamics is that the safety factor  $q$  is driven below 1 by the effect of core heating, which increases the temperature, thereby increasing the plasma conductivity  $\sigma \sim T_e^{\frac{3}{2}}$  and causing an inward current diffusion. This condition destabilises the (1, 1) mode, which triggers a rapid crash of the kinetic and  $q$  profiles via magnetic reconnection. Subsequently, the profiles are gradually reestablished due to continued heating and fuelling, leading to the next crash and forming a repeating cycle.

Recently, an integrated model of sawtooth cycles [2] has been developed and implemented in the ASTRA transport code [3–5]. In this model, the sawtooth crash time is predicted through the Porcelli onset criteria [6]. At the crash time, the current and  $q$  profiles are modified through the Flat Current model [7] to obtain the post-crash profiles. The crash of the electron density, electron temperature, ion temperature

and fast ion density are obtained through sawtooth-induced transport coefficients  $D_e, \chi_{e,i}, D_{fast} \sim \frac{r_1^2}{\tau_{crash}}$ , where  $\tau_{crash}$  is the duration of a sawtooth crash — on the order of  $\sim 20 \mu\text{s}$  to  $\sim 200 \mu\text{s}$  for ASDEX Upgrade [8–10] — and  $r_1$  is the minor radius of the  $q = 1$  surface. Since the momentum diffusivity is assumed to be proportional to the ion heat conductivity, an increase in the ion conductivity causes also a crash of the rotation profile. After the crash, the profiles recover through heating, fuelling and current drive, and the rate of recovery of the profiles is set by the transport coefficients, which are calculated by TGLF-SAT2 [11, 12] for the turbulent contribution and NCLASS [13] for the neoclassical one. With the TGLF settings of [12], which are meant to better capture Kinetic Ballooning modes (KBMs) in high  $\beta$  scenarios, it was found that TGLF predicts large transport around the  $q = 1$  surface, compared to the transport obtained through a power balance on the experimental profiles, which can significantly affect the recovery phase and the pre-crash profiles for the subsequent crash.

Several hypotheses were proposed to explain the high levels of turbulence predicted by TGLF, such as the effects of fast ions, the breaking of axisymmetry due to

\*Email: federico.stefanelli@ipp.mpg.de

the MHD activity present during the recovery phase, or numerical issues arising from calculating turbulent fluxes in regions of low shear as in a sawtooth plasma core. To obtain gradients compatible with the experimental profiles, an additional term localized around the  $q = 1$  surface was added to the poloidal flow, in order to suppress turbulence through  $E \times B$  shear. This additional term was qualitatively compatible in shape to the one driven by Toroidal Alfvén Eigenmodes (TAEs) [14], which were present in the discharges analyzed, or by self-interacting turbulent modes at rational surfaces, for which the threshold for zonal flow generation can be significantly reduced by fast-ion dilution [15]. The amplitude of this additional poloidal flow component was kept as free parameter, as it was primarily meant to be one way to obtain the correct gradients and thus validate the sawtooth model predictions. It is worth mentioning that also fishbones are present in the analyzed discharge and the fishbone-driven radial electric field was included through a first-principle model, but it was found to be too small to have a significant effect on turbulence. In the work here presented, the growth rates calculated by TGLF at the  $q = 1$  surface are compared to the linear calculations of GENE [16], to better understand the origin of the large transport predicted by TGLF. The growth rates calculated by GENE are found to agree with those predicted by TGLF with the KBM settings of [12], for  $k_y \rho_s > 0.1$ . However, with these settings TGLF also finds modes with large growth rates and frequencies for  $k_y \rho_s < 0.1$ , which are not found by GENE. On the other hand, the default settings of TGLF-SAT2 [11] are found to predict a turbulent transport closer to the one needed to reproduce the experiment, but with growth rates up to one order of magnitude smaller than those found by GENE and by TGLF with KBM settings. These results support the hypothesis of turbulence stabilisation mechanisms missing in TGLF and in the GENE calculations, as those mentioned above, which are only compensated by the low growth rates found by TGLF with default settings. The comparison between GENE and TGLF is shown in Section 2, as well as the simulation results of discharge #34664, for which both the standard settings of TGLF-SAT2 and the KBM settings with  $k_y \rho_s \geq 0.15$  are tested. Finally, a conclusion section summarises the results of this work.

## 2. Results

In the following, the comparison between the linear, local calculations of GENE and TGLF at the  $q = 1$  surface is discussed for profiles in the saturation phase of a sawtooth cycle of discharge #34664. The difference in settings between the default version of TGLF and the one aiming at better capturing KBMs is shown in Table 1.

Parameter	Default	KBM
FILTER	2.0	-0.1
WIDTH	1.65	3.0
WIDTH_MIN	0.3	-0.3
ALPHA_ZF	1	-1
USE_MHD_RULE	False	True

Table 1: Settings difference between the default version of TGLF-sat2 and the settings aiming at better capturing Kinetic Ballooning modes.

Figure 1 shows the comparison of the growth rates and frequencies of the fastest growing modes as function of  $k_y \rho_s$  between GENE, TGLF with default settings and TGLF with KBM settings. It can be seen that TGLF with the KBM settings agrees with GENE better than with the default settings for  $k_y \rho_s > 0.1$ , with the case with default settings calculating growth rates up to one order of magnitude smaller than those of GENE and of TGLF with KBM settings. However, both versions of TGLF predict two modes at  $k_y \rho_s < 0.1$ , which are not found by GENE. The predicted growth rates of these modes are significantly higher in the case with the KBM settings. As far as the frequency of these modes are concerned, the one predicted by TGLF with default settings is  $\sim 0$ , while  $|\omega_a/c_s| > 1$  for the case with the KBM settings.

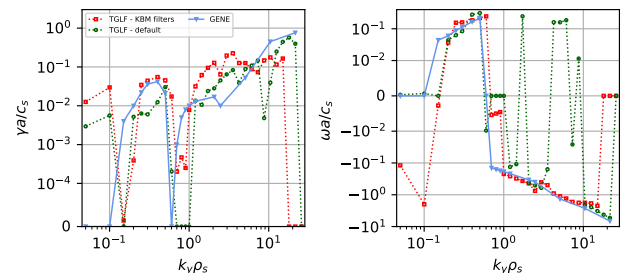


Figure 1: Comparison of the linear growth rates of the most unstable mode as function of  $k_y \rho_s$  for GENE (blue), TGLF with default settings (green) and TGLF with KBM settings (red).

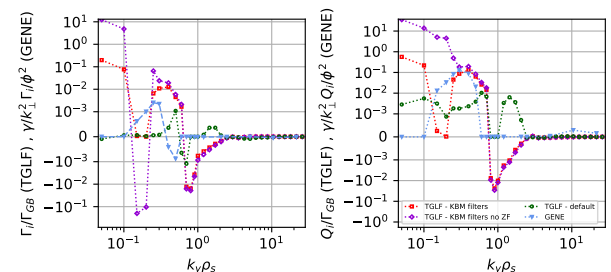


Figure 2: Comparison of the ion particle transport (left) and ion heat transport (right) as function of  $k_y \rho_s$  for GENE (blue), TGLF with default settings (green), TGLF with KBM settings (red) and TGLF with KBM settings and ALPHA\_ZF = 1 (purple).

The higher growth rates and frequencies of the low

$k_y \rho_s$  modes result in a significant increase in the predicted transport at low  $k_y \rho_s$  for TGLF with KBM settings, compared to the case with default settings and to GENE, as shown in Figure 2. It must be noted that the flag ALPHA\_ZF, the zonal flow mixing coefficient, equal to  $-1$ , instead of  $1$ , should strongly reduce the growth rates of the modes at the lowest  $k_y \rho_s$  by avoiding finding unphysical peaks in  $\gamma/k_y$  and thus the predicted transport, compared to the case with ALPHA\_ZF =  $1$ . Without this, the growth rates and transport predicted by TGLF with KBM settings are even higher, as can be seen in the case of transport in Figure 2. However, even without considering the modes at  $k_y \rho_s \leq 0.1$ , the transport predicted by TGLF with default settings is much lower than the one with KBM settings, with the latter qualitatively agreeing with GENE.

Based on the results presented above, the sawtooth model of [2] is tested in ASTRA with the default settings and with the KBM settings of TGLF-SAT2, for which  $k_y \rho_s \geq 0.15$ . The simulation setup is the same as the one of the simulations of the same discharge discussed in [2], apart from the TGLF settings. As in [2], the simulated discharge is #34664.

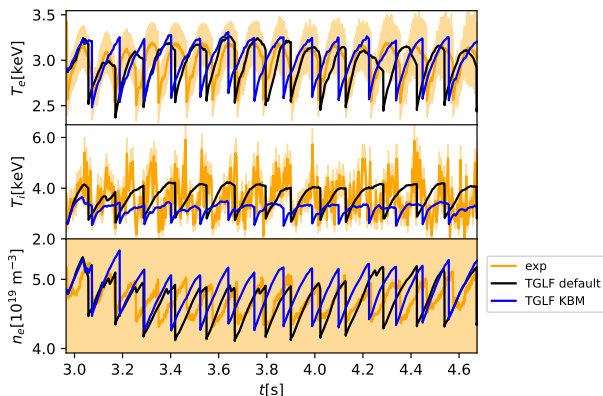


Figure 3: Comparison of the time traces of  $T_e$ ,  $T_i$  and  $n_e$  on axis of discharge #34664 between the model with default settings of TGLF (black), with the KBM settings (blue) and the experimental ones (orange).

Figure 3 shows the time traces of  $T_e$ ,  $T_i$  and  $n_e$  on axis for the case employing TGLF with default settings (black) and with KBM settings (blue), compared to the experimental ones, obtained from Integrated Data Analysis (IDA) [17] for  $T_e$  and  $n_e$  and Charge Exchange Recombination Spectroscopy (CXRS) for  $T_i$ . The average sawtooth period in the simulation with the default settings of TGLF is  $0.12 \pm 0.01$  s, within the error bars of the experimental one of  $0.11 \pm 0.01$  s. Also the recovery rate of the profiles after a sawtooth crash agrees with the experimental one, as well as the maximum value reached by all three variables before a sawtooth crash. On the other hand, the simulation employing the KBM settings of TGLF-SAT2 with  $k_y \rho_s \geq 0.15$  results in an underestimated  $T_i$ . It is worth mentioning that in the original setup of

the simulations used in [2] an additional component of the tungsten concentration was added to describe the tungsten accumulation observed in the experiment. This component had to be removed for the simulation with the KBM settings of TGLF, as the tungsten radiation, combined with the high turbulent transport, would not have allowed the  $T_e$  profile to recover, as shown in Figure 4. A significantly lower core  $T_e$  strongly influences both the prediction of ITG turbulence, due to the different ratio of  $T_e/T_i$ , and of the sawtooth model, as it affects current diffusion through a reduced conductivity  $\sigma \sim T_e^{3/2}$ . The underestimation of  $T_i$  for TGLF with KBM settings, despite its good agreement with GENE, supports the idea that turbulence stabilisation mechanisms could be missing in TGLF and in the GENE calculations, as discussed in [2] and in the introduction, which are only compensated by the low growth rates found by TGLF with the default settings.

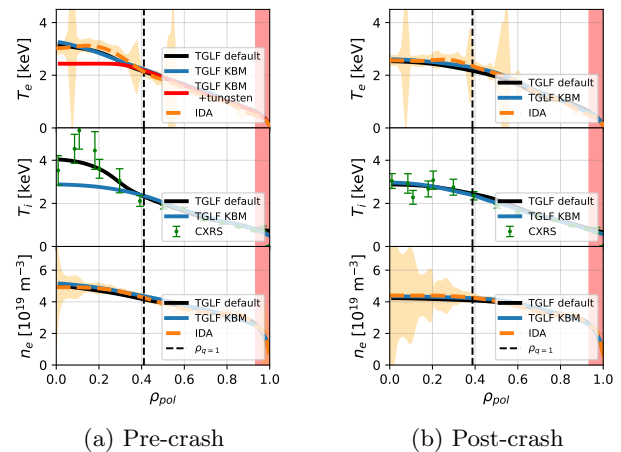


Figure 4: Pre-crash profiles (a) and post-crash profiles (b) of  $T_e$ ,  $T_i$  and  $n_e$  for discharge #34664. The position of the  $q = 1$  surfaces is represented by the dashed, black line, while the simulation boundary is represented by the shaded red area.

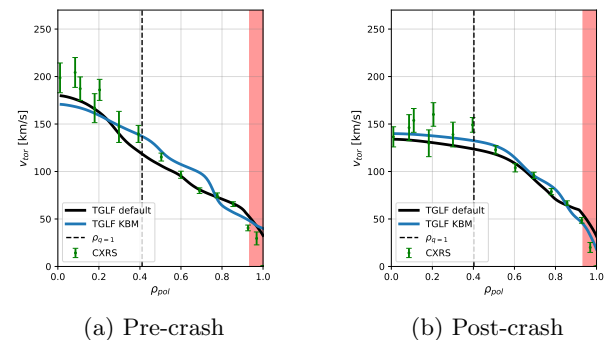


Figure 5: Pre-crash profiles (a) and post-crash profiles (b) of the toroidal rotation profile for discharge #34664. The position of the  $q = 1$  surfaces is represented by the dashed, black line, while the simulation boundary is represented by the shaded red area.

Figure 4 shows the pre- and post-crash profiles at  $t = 4.0$  s for the case of TGLF with default settings (black) and KBM settings (blue), while Figure 5 shows the toroidal rotation profile. In all cases, the simulated profiles fall within the error bars of the experimental data for the case with default settings, but the ion temperature is strongly underestimated in the case employing the KBM settings, as well as the electron temperature, if tungsten accumulation is considered.

### 3. Conclusions

In this work, the results of gyrokinetic calculations of GENE are compared to those of TGLF-SAT2, for which both default settings and settings aiming at better describing Kinetic Ballooning Modes (KBM) are used. TGLF with KBM settings is found to agree with GENE better than TGLF with default settings for  $k_y \rho_s > 0.1$ , with the latter significantly underestimating the growth rates of the dominant turbulent modes for  $k_y \rho_s < 1$ . However, TGLF with KBM settings finds modes with large growth rates and frequencies for  $k_y \rho_s < 0.1$ , which are not found by GENE and significantly contribute to the total turbulent flux.

Both versions of TGLF are tested in a recently developed sawtooth cycle integrated model, with  $k_y \rho_s \geq 0.15$  for the case employing the KBM settings. It is found that with the default settings the model yields an excellent agreement with the experimental data, while the case with KBM settings leads to a significantly underestimated ion temperature. The underestimation of  $T_i$  for TGLF with KBM settings, despite the good agreement with the linear calculations of GENE, hints at the possibility of missing turbulence suppression mechanisms, which are only compensated by the low growth rates found by TGLF with default settings.

These results are significant, since on one hand they support the validity of the newly developed settings of TGLF for  $k_y \rho_s > 0.1$  in the core of AUG plasmas, while on the other hand show the need of a better treatment of the modes at  $k_y \rho_s < 0.1$ . Furthermore, the agreement between TGLF with KBM settings and GENE for  $k_y \rho_s > 0.1$ , but the disagreement with the experimental profiles of sawtooth discharges, supports the hypothesis that additional physics must be included in the turbulent calculations around the  $q = 1$  surface. One possibly missing effect is the reduction of the threshold of zonal flow generated by self-interacting turbulent modes through fast-ion dilution [15]. In the future, global, nonlinear GENE simulations could be run to compare the nonlinear turbulent fluxes to those predicted by TGLF, and to assess the effects of fast-ion dilution on the zonal flow generation. Other possibly missing mechanisms are the effects of the constant MHD activity in the core between sawtooth crashes, which can influence turbulence in multiple ways. For instance, TAEs and fishbones can drive additional components of the radial

electric field  $E_r$ . In the case of fishbones, the model employed in the simulations here presented [2] predicts only a minor contribution to the total  $E_r$ , but a kinetic description of the mode is currently missing and could significantly affect the driven  $E_r$ . Finally, MHD activity could break axisymmetry, which is assumed both by TGLF and GENE, although one would typically expect an increase in transport when axisymmetry is broken.

### Data availability statement

The data supporting the results of this work is available from the authors upon reasonable request.

### Acknowledgements

This work has been carried out within the framework of the EUROfusion Consortium, funded by the European Union via the Euratom Research and Training Programme (Grant Agreement No 101052200-EUROfusion). Views and opinions expressed are however those of the authors only and do not necessarily reflect those of the European Union or the European Commission. Neither the European Union nor the European Commission can be held responsible for them.

### References

- [1] von Goeler S. *et al* 1974 *Phys. Rev. Lett.* **33** 1201–1203
- [2] Stefanelli F. *et al* 2026 *Nucl. Fusion* **66** 076003
- [3] Pereverzev G. 1991 Tech. rep. IPP Report No IPP 5/42
- [4] Fable E. *et al* 2013 *Plasma Phys. Control. Fusion* **55** 074007
- [5] Tardini G. *et al* 2026 *Plasma Phys. Control. Fusion* **68** 065024
- [6] Porcelli F. *et al* 1996 *Plasma Phys. Control. Fusion* **38** 2163–2186
- [7] Fischer R. *et al* 2019 *Nucl. Fusion* **59** 056010
- [8] Letsch A. *et al* 2002 *Nucl. Fusion* **42** 1055–1059
- [9] Igochine V. *et al*, *35th EPS Conference on Plasma Physics and 10th International Workshop on Fast Ignition of Fusion Targets* (European Physical Society) 2008.
- [10] Samoylov O. *et al* 2022 *Nucl. Fusion* **62** 074002
- [11] Staebler G. *et al* 2021 *Nucl. Fusion* **61** 116007
- [12] Najlaoui A. *et al* 2025 *Plasma Phys. Control. Fusion* **67** 045016
- [13] Houlberg W. A. *et al* 1997 *Phys. Plasmas* **4** 3230–3242
- [14] Chen L. *et al* 2024 *Nucl. Fusion* **65** 016018
- [15] Brioschi D. *et al* 2026 *Nucl. Fusion* **66** 076004
- [16] Görler T. *et al* 2011 *Journal of Computational Physics* **230** 7053–7071
- [17] Fischer R. *et al* 2010 *Fusion Sci. Technol.* **58** 675–684